Design of a resonant-cavity-enhanced GaInAsSb/GaSb photodetector

2004 Semicond. Sci. Technol. 19 690

(http://iopscience.iop.org/0268-1242/19/6/005)

INSTITUTE OF PHYSICS PUBLISHING SEMICONDUCTOR SCIENCE AND TECHNOLOGY
Semicond. Sci. Technol. **19** (2004) 690–694 PII: S0268-1242(04)71447-9

Design of a resonant-cavity-enhanced GaInAsSb/GaSb photodetector

Li Jun, Song Hang, Yixin Jin, Jiang Hong, Guoqing Miao and Haifeng Zhao

Key Laboratory of Excited State Processes, Changchun Institute of Optics, Fine Mechanics and Physics, Chinese Academy of Sciences, Changchun 130031, People's Republic of China

E-mail: snmocvd@public.cc.jl.cn

Received 5 November 2003, in final form 22 January 2004
Published 8 April 2004
Online at stacks.iop.org/SST/19/690 (DOI: 10.1088/0268-1242/19/6/005)

Abstract
A resonant-cavity-enhanced (RCE) PIN photodetector has high bandwidth and high sensitivity compared with traditional PIN photodetectors. In this paper, the structure of a RCE GaInAsSb/GaSb photodetector has been designed so that the light is incident from the substrate. The top reflector for this structure is made of 9.5–15.5 periods of InAs/GaSb quarter wave stacks (QWS) and the bottom reflector is composed of three periods of SiO_2/Si QWS. An antireflection coating with more than 99% transmissivity is deposited on the substrate surface. A simulation shows that the quantum efficiency could be more than 90% at the operating wavelength 2.4 μm. The device has two spectral response peaks, which could make the device function as a double-colour detector.

1. Introduction

The 2–5 μm mid-infrared wavelength region is of great interest for a wide range of applications such as optical communications, environmental protection and military applications. GaInAsSb quaternary alloys lattice-matched to GaSb are ideal for use as detectors in the 1.7–4.3 μm wavelength range because of their high sensitivity and high operating temperature [1–3]. In a traditional PIN photodetector, the incident light passes through the absorbing layer only once and the quantum efficiency is low. Making the absorbing layer thicker to increase the quantum efficiency, will reduce the bandwidth of the device accordingly. So there is a trade-off between quantum efficiency and bandwidth in device design. To resolve this problem, a resonant-cavity-enhanced (RCE) photodetector has been developed [4]. In this device, a PIN photodetector is put inside a Fabry–Perot cavity and the incident light has more than one absorbing path inside the absorbing region due to multiple reflections, as shown in figure 1. Because of the large amplification of the resonant optical field within this cavity, a very thin absorbing layer can reach high quantum efficiency as well as a high speed of response. Hence, a RCE photodetector with quantum efficiency close to unity may be achieved.

The study of RCE photodetectors has been mainly concentrated on Ge/GeSi, InGaAsP/InP and InGaAs/InP (GaAs) photodetectors up to now and a device with more than 100 GHz bandwidth has been demonstrated [5–10]. But GaInAsSb/GaSb RCE photodetectors have few reports. Yan Shi *et al* [11] reported a GaInAsSb/AlGaAsSb RCE photodetector grown by MBE in 1998. In their study, the bottom reflector is made of AlAsSb/GaSb quarter wave stacks (QWS). It is well known that the growth of binary compounds is easier than that of the ternary or the quaternary. In this paper, we have extended the application of RCE structure to a GaInAsSb/GaSb photodetector operating at 2.4 μm. The structure of GaInAsSb/GaSb RCE photodetector based on InAs/GaSb QWS has been designed and the quantum efficiency has been calculated.

2. Analysis

2.1. Materials

For a typical RCE photodetector, the reflector grown on a substrate is made of QWS which are composed of two semiconductors grown alternately. The difference between the refractive indices of the two semiconductors is considered to be large enough so that the period number of QWS for high reflectivity can be reduced. The energy gap of the two semiconductors should be larger than the photon energy of the incident light to reduce the absorption by the QWS. The

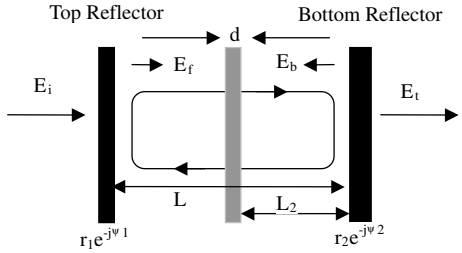

Figure 1. Schematics of the Fabry–Perot cavity model. The shaded region is used to simulate the absorbing region placed in the cavity.

two semiconductors must be lattice-matched to each other and also to the substrate to reduce the density of interface states. InAs/GaSb heterostructure match very well and their refractive indices at 2.4 μm are 3.755 and 3.516, respectively. These show that InAs/GaSb QWS may be used as the reflector in a GaInAsSb/GaSb RCE photodetector. But the photon energy at the operating wavelength 2.4 μm is larger than the energy gap of InAs and the absorption coefficient of intrinsic InAs is more than 10^4 cm^{-1} at the operating wavelength, which results in an increase in the absorption by the QWS and a decrease in the quantum efficiency. However, the semiconductors of the QWS are generally doped heavily to reduce the series resistance. According to the Bustein shift [12], the absorption edge of heavily doped semiconductor would move towards the short wavelength region. For example, the absorption coefficient of doped n$^+$-InAs with a carrier concentration of 3.8×10^{18} cm^{-3} is about 4×10^2 cm^{-1} [13]. If the InAs is heavily doped and its total length is not more than several micrometres, only a little incident light will be absorbed in the QWS, as shown below. The growth of InAs/GaSb heterostructure has already been reported [14]. So a reflector which is made of InAs/GaSb QWS is feasible in a GaInAsSb/GaSb RCE photodetector operating at 2.4 μm. The composition of GaInAsSb can be calculated with linear interpolation [15]. For operating at 2.4 μm and lattice-matching to GaSb, the alloy $Ga_{0.75}In_{0.25}As_{0.02}Sb_{0.98}$ is selected.

2.2. Reflectivity and reflection phase shift of reflector

The reflectivity and reflection phase shift of a reflector made by QWS can be calculated by the transfer matrix method [16]. The lightwave transmitting through the film can be described by the characterized matrix as

$$M = \begin{bmatrix} \cos(k_0 h) & \mathrm{i}\sin(k_0 h)/\Gamma \\ \mathrm{i}\Gamma\sin(k_0 h) & \cos(k_0 h) \end{bmatrix} \tag{1}$$

where

$$\Gamma = \sqrt{\frac{\varepsilon_0}{\mu_0}} n\cos\theta \qquad k_0 h = nd\cos\theta \cdot 2\pi/\lambda. \tag{2}$$

n and d are refractive index and the thickness of the film, respectively. θ is the refractive angle and λ is the wavelength of incident light. As the light is normal incident, θ is zero. The characterized matrix of multilayer films can be expressed by

$$M = M_1 \times M_2 \times \cdots \times M_n = \begin{bmatrix} m_{11} & m_{12} \\ m_{21} & m_{22} \end{bmatrix}. \tag{3}$$

Then the reflectance r and reflectivity R can be obtained, respectively, by the following formulae:

$$r(\lambda) = \frac{\Gamma_0 m_{11} + \Gamma_0\Gamma_s m_{12} - m_{21} - \Gamma_s m_{22}}{\Gamma_0 m_{11} + \Gamma_0\Gamma_s m_{12} + m_{21} + \Gamma_2 m_{22}} \tag{4}$$

$$R(\lambda) = r(\lambda) \times r(\lambda)^* \tag{5}$$

where subscripts 0 and s represent the incident medium and the substrate medium, respectively. The reflection phase shift of the reflector is given by

$$\psi(\lambda) = -\arg[r(\lambda)]. \tag{6}$$

2.3. Quantum efficiency

For the model shown in figure 1, the quantum efficiency of the RCE photodetector can be expressed by [17]

$$\eta = \left\{[1 + R_2(\lambda)\,\mathrm{e}^{-\alpha(\lambda)d}]\Big/\Big[1 - 2\sqrt{R_1(\lambda)R_2(\lambda)}\,\mathrm{e}^{-a(\lambda)d} \times \cos(2\beta L + \psi_1(\lambda) + \psi_2(\lambda)) + R_1(\lambda)R_2(\lambda)\,\mathrm{e}^{-2\alpha(\lambda)d}\Big]\right\} \times (1 - R_1(\lambda))(1 - \mathrm{e}^{-\alpha(\lambda)d}) \tag{7}$$

where α is the absorption coefficient, d is the thickness of the absorbing layer and R_1, R_2 are reflectivity of the top reflector and the bottom reflector, respectively. ψ_1 denotes the reflection phase shift of the top reflector and ψ_2 denotes that of the bottom reflector. β is the propagation constant and L is the effective length of the cavity. The maximum quantum efficiency occurs when $\cos(2\beta L + \psi_1 + \psi_2) = 1$. It then follows that [17]

$$\eta_p = \left\{\frac{(1 + R_2\,\mathrm{e}^{-\alpha d})}{(1 - \sqrt{R_1 R_2}\,\mathrm{e}^{-\alpha d})^2}\right\} \times (1 - R_1)(1 - \mathrm{e}^{-\alpha d}). \tag{8}$$

The maximum η_p can be obtained at $R_1 = R_2\,\mathrm{e}^{-2\alpha d}$. At the off-resonant points, that is when $2\beta L + \psi_1 + \psi_2 = (2n + 1)\pi$, $(n = 1, 2, \ldots)$, the field amplitude of the light between the two end reflectors decreases due to the destructive interference of forward and backward travelling waves, resulting in suppressed quantum efficiency; for a high Q resonant cavity in particular the quantum efficiency will be lower [17]. If the absorption of the top reflector is taken into account, $(1 - R_1)$ in (7) and (8) should be replaced by $(1 - R_1 - A)$, where

$$A = (1 - R_1) \times (1 - \mathrm{e}^{-\alpha_D d_D}) \tag{9}$$

is the absorption percentage of the incident light, where α_D, d_D are the effective absorption coefficient and the effective absorption length of top QWS, respectively. Then the quantum efficiency can be expressed by

$$\eta_{\mathrm{eff}} = \eta \cdot \mathrm{e}^{-\alpha_D d_D}. \tag{10}$$

This shows that the quantum efficiency will decrease as an exponential function of the thickness and absorption of the top reflector. For a RCE photodetector the standing wave effect must be considered. Then the absorption coefficient α of absorbing layer should be replaced by [4]

$$\alpha_{\mathrm{eff}} = \alpha \cdot \mathrm{SWE} \tag{11}$$

where

$$\mathrm{SWE} = 1 + \frac{2r_2}{\beta d\left(1 + r_2^2\right)}[\sin\beta d\cos(2\beta L_2 + \beta d + \psi_2)] \tag{12}$$

where L_2 symbolizes the distance from the bottom reflector to the absorbing layer, and r_2 is the reflectance of the bottom reflector.

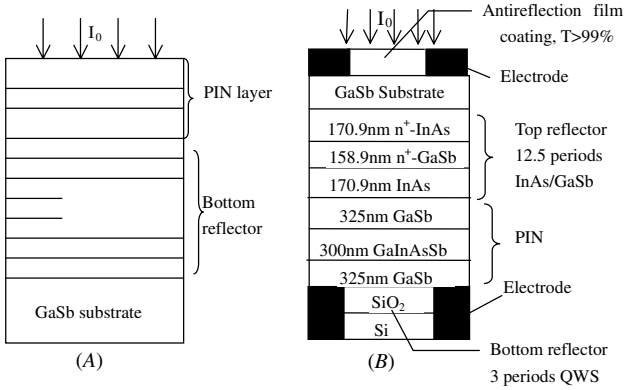

Figure 2. The structures of the devices for different designs. (*A*) The structure of a typical RCE PD. The resonant cavity is between the air–semiconductor interface and the substrate. (*B*) Structure of the GaInAsSb p-i-n RCE PD in which the light is incident from the substrate.

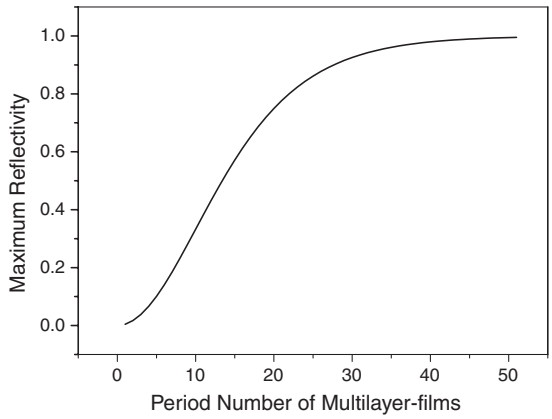

Figure 3. Reflectivity of InAs/GaSb QWS as a function of periods.

3. Structure of device

The typical RCE photodetector structure is shown in figure 2(*A*). If this structure is selected for a RCE GaInAsSb/GaSb photodetector, the top reflector generally uses the air–semiconductor interface whose reflectivity is about 34%, and the bottom reflector is made of InAs/GaSb QWS whose reflectivity as a function of the period number is shown in figure 3. It can be seen in figure 3 that the reflectivity of 27.5, 33.5, 45.5 periods of InAs/GaSb QWS is 90%, 95% and 99%, respectively. QWS with so many periods will make the growth of a high quality reflector difficult and increase the series resistance. To resolve this problem, the structure shown in figure 2(*B*) has been designed. In this structure the light is incident from the substrate. The antireflection coating with more than 99% transmissivity should be deposited on the substrate surface. The top reflector is made of InAs/GaSb QWS and the bottom reflector is composed of three periods of Si/SiO_2 QWS which has 99.4% reflectivity. The peak reflectivity of the top reflector is 33.2%, 48.1% and 61.3% at the operating wavelength 2.4 μm with 9.5, 12.5 and 15.5 periods of QWS, respectively, as shown in figure 3. The curves of quantum efficiency as a function of αd at different R_1 are shown in figure 4. From these curves it can be seen that all the quantum efficiency peaks are more than 99% if the absorption

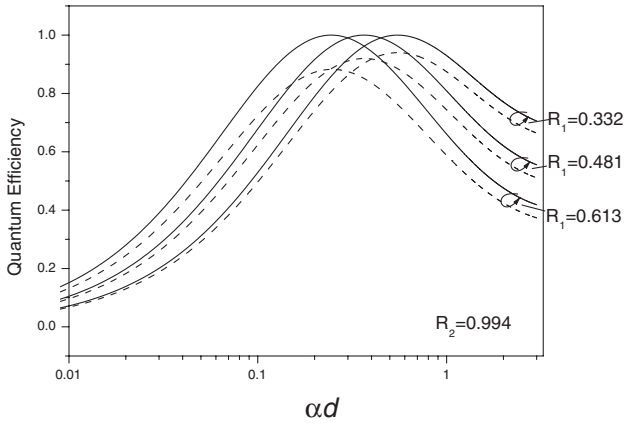

Figure 4. The dependence of quantum efficiency on αd for different R_1. The solid line is when the absorption of the top reflector is neglected while the dot line is included.

of the top reflector is neglected. To obtain more accurate quantum efficiency the absorption of the top reflector is considered. As the device operates at 2.4 μm, the thickness of InAs and GaSb is easily calculated as 170.9 nm and 158.9 nm, respectively. Because of the multiple reflections in the QWS, the absorption of the top reflector is difficult to calculate accurately. Neglecting the absorption of GaSb (it is small compared with the absorption of InAs) and replacing α_D and d_D in formula (8) by the absorption coefficient and the thickness of InAs are adopted to approximately calculate the absorption of the top reflector. As the absorption of the top reflector is taken into account, the quantum efficiency decreases to 88.3%, 91.2% and 93.5% for 15.5, 12.5 and 9.5 periods of InAs/GaSb QWS, respectively, as shown in figure 4. Furthermore, the InAs/GaSb heterojunction has II-type energy band structure. It is noted that the heterojunction will have semimetal properties if the thickness of each period in InAs/GaSb multilayer films is more than 17 nm [18]. As the thickness of InAs and GaSb in the QWS is 170.9 nm and 158.9 nm, respectively, obviously the heterojunction has semimetal properties, which would make the series resistance of the QWS very low, resulting in reduced the voltage on the QWS and improving the performance of the device. This shows that the structure represented by figure 2(*B*) is feasible and easy to grow. The thickness of each layer is given in figure 2(*B*), in which the cavity thickness is given for a device with 12.5 periods of top QWS.

4. Results and discussion

To simplify the preparation of the device, the structure shown in figure 2(*B*) is selected. Some properties of the device are calculated to estimate its performance. As the value of αd depends strongly on the incident light wavelength, the dependence of the absorption coefficient on the wavelength should be taken into account to calculate the variation of the quantum efficiency with the wavelength. To the best of our knowledge the absorption coefficient of GaInAsSb has not been reported. Adachi [19] has given InAs and GaSb absorption coefficients, from which it can be seen that the absorption coefficients of InAs and GaSb are consistent with

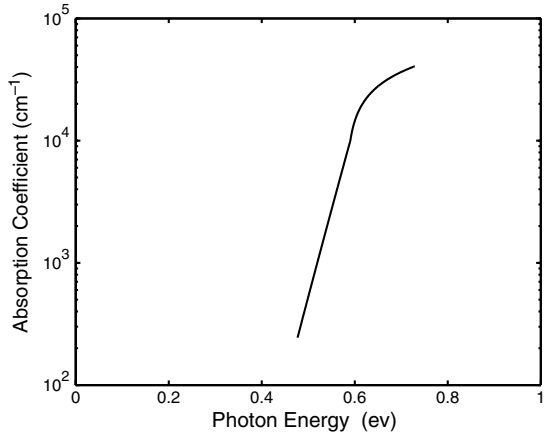

Figure 5. The simulated GaInAsSb absorption coefficient.

the relationship of the absorption coefficient of a direct band semiconductor on the wavelength, which can be expressed as follows [20]:

$$\alpha(h\upsilon) = \begin{cases} A(h\upsilon - E_g)^{1/2}, h\upsilon > E_g \\ B \cdot \exp(c \cdot \upsilon), h\upsilon < E_g \end{cases} \quad (13)$$

Table 1. Optical parameters of materials used in calculation.

	GaInAsSb	GaSb	InAs	Si	SiO_2
Refractive index (at 2.4 μm)	3.7	3.755	3.516	1.46	3.46
Absorption coefficient ($\times 10^4$ cm^{-1})	1	0	0.04 (3.8×10^{18} cm^{-3} n$^+$-doped)	0	0

where A, B, and c are coefficients. For calculating approximately, it is assumed that the absorption coefficient of GaSb-rich GaInAsSb follows the relation (13) and its variation with wavelength is similar to that of GaSb. Generally, it is assumed that the absorption coefficient is approximately 1×10^4 cm^{-1} near the absorption edge for direct band gap III–V semiconductors [11]. Based on this, the absorption coefficient of GaInAsSb has been simulated, as shown in figure 5. The optical parameters of materials used in the calculation are shown in table 1. As the refractivity variations of both InAs and GaSb from 2 to 2.9 μm are small [21], the dispersion of refractivity is neglected during calculation. Some properties of the designed device including the reflection phase shift and the reflectivity of QWS are shown in figures 6(*A*) and (*B*), respectively. The graphs show that the variation of the bottom reflector's reflectivity and the phase shift with wavelength are

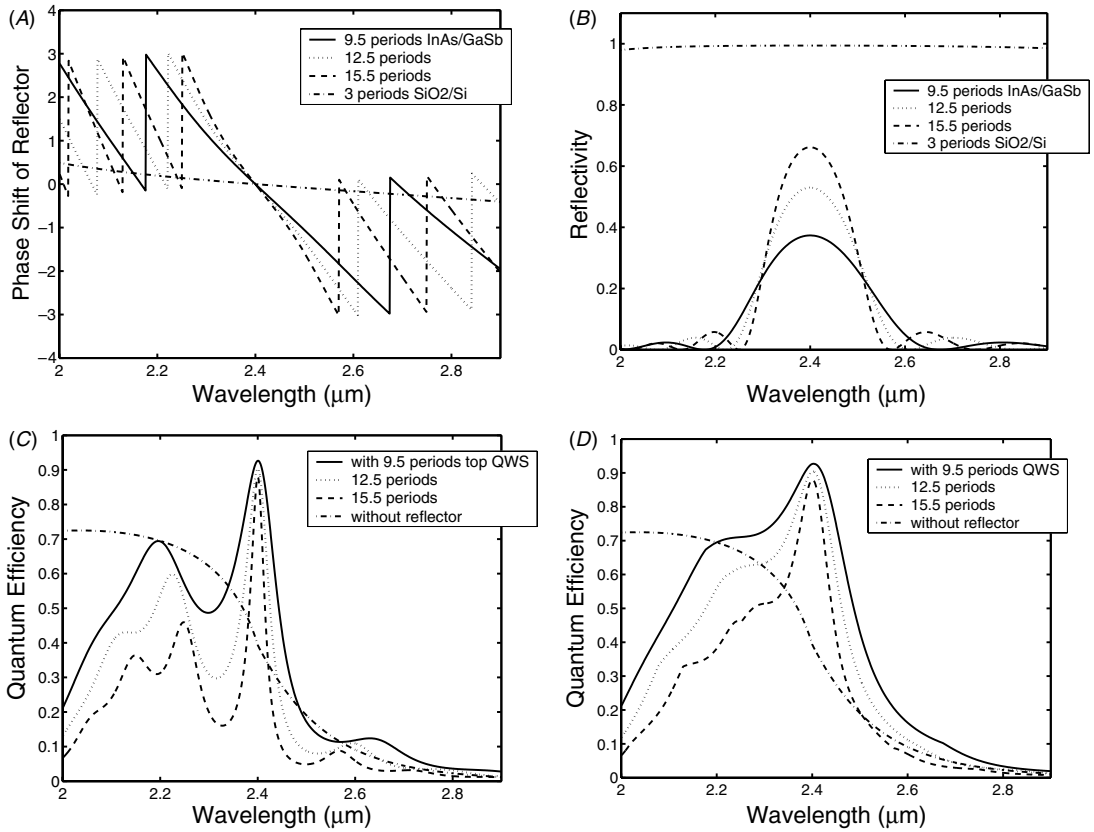

Figure 6. Calculated properties of the designed device. (*A*) The phase shift of the reflector. (*B*) The reflectivity of the reflector for different numbers of periods of InAs/GaSb QWS and three periods of Si/SiO_2. (*C*) The quantum efficiency η as a function of wavelength. The absorption of the top reflector is taken into account for the calculation. The dependence of η of 500 nm-absorbing layer device without a reflector on wavelength is also shown for comparison. (*D*) The quantum efficiency η as a function of wavelength. The absorption of the top DBR is taken into account for the calculation and the phase shift of the reflector is neglected. The dependence of η of 500 nm-absorbing layer device without a reflector on wavelength is also shown for comparison.

minimal. However, the top reflectors have high reflectivity in a very narrow wavelength range and the phase shifts vary from 0 up to 3 periodically and have sudden transitions at the wavelength with minimum reflectivity. Figure 6(*C*) shows the variation of quantum efficiency with wavelength. The cut-off wavelength is in the range of 2.48–2.56 μm and is altered by a different R_1. Each curve of the quantum efficiency has two peaks, which correspond to the maximum and minimum reflectivity of the top reflector. These show that the devices will have two spectral response peaks and could function as a double-colour detector. Figure 6(*D*) shows the quantum efficiency of the devices when the phase shifts of the top reflector are neglected. Comparing figure 6(*C*) with 6(*D*), the quantum efficiency is obviously suppressed between the two peaks in figure 6(*C*), which is dominated by the phase shift of the top reflector. As the reflectivity of the top reflector decreases from the peak at 2.4 μm down to zero at the short wavelength region, the phase shift is from 0 up to about 3, which makes the cavity tend to the off-resonant points mentioned before, resulting in suppressed quantum efficiency, in particular, the higher the reflectivity of the top reflector, the lower the quantum efficiency. Therefore, another peak of quantum efficiency occurs at the minimum reflectivity of the top reflector. The quantum efficiency of nearly 2 μm in figure 6(*C*) reduced rapidly, which is caused by the high absorption of the QWS. It is apparent that the device with 9.5 periods of QWS has more than 40% quantum efficiency in the range from 2.06 to 2.45 μm. However, the devices with 12.5 and 15.5 periods of InAs/GaSb QWS have more than 40% quantum efficiency only near the two peaks. As shown in figure 4, the thickness of the absorbing layer may reduce as the reflectivity of the top QWS increases, which will increase the bandwidth of the device. These show that the device with 9.5 periods of InAs/GaSb QWS will have a broad spectral response range while one with 12.5 or more periods QWS will have higher bandwidth.

5. Conclusion

We have designed a structure for a RCE photodetector based on a GaInAsSb/GaSb heterojunction. In this structure, the top reflector is made of InAs/GaSb QWS and the bottom reflector is composed of three periods of SiO_2/Si QWS. The light is incident from the substrate which has an antireflection coating. The quantum efficiency of the designed devices has been simulated in a closed analytical form that includes the structure parameters of the photodetector. The dependences of QWS reflectivity and reflection phase shifts as well as the absorption coefficient of GaInAsSb on wavelength have been considered. It is found that the reflection phase shifts affect the quantum efficiency greatly. The maximum quantum efficiency of more than 90% can be obtained at 2.4 μm if the top reflector is made of 9.5–12.5 periods of InAs/GaSb. The devices have two spectral response peaks, which will make the device function as a double-colour detector. The device with 9.5 periods of InAs/GaSb QWS will have more than 40% quantum efficiency from 2.06 to 2.46 μm, due to which the device has a broad spectral response range. As the number of periods increases, the device bandwidth will increase and the maximum quantum efficiency will decrease.

Acknowledgment

This work is supported by National Natural Science Foundation of China under grants nos 60177014, 50072030 and 50132020.

References

[1] Tournie E *et al* 1991 *Electron. Lett.* **27** 1237–9
[2] Zhang B *et al* 1995 *Electron. Lett.* **31** 830–2
[3] Yuan T *et al* 2003 *Microelectron. J.* **34** 305–12
[4] Selim Ünlü M and Strite S 1995 *J. Appl. Phys.* **78** 607–39
[5] Selim Ünlü M *et al* 1990 *Appl. Phys. Lett.* **57** 750–2
[6] Kuchibhotla R *et al* 1993 *Appl. Phys. Lett.* **62** 2215–7
[7] Dentai A G *et al* 1991 *Electron. Lett.* **27** 2125–7
[8] Gvozdić D M *et al* 2000 *Semicond. Sci. Technol.* **15** 630–7
[9] Bourdoucen H and Jervase J A 2001 *Semicond. Sci. Technol.* **16** 581–3
[10] Onat B M *et al* 1998 *IEEE Photon. Technol. Lett.* **10** 707–9
[11] Shi Yan *et al* 1998 *IEEE Photon. Technol. Lett.* **10** 258–60
[12] Moss T S *et al* 1973 *Semiconductor Opto-Electronics* (London: Butterworths)
[13] Dixon J R *et al* 1961 *Phys. Rev.* **123** 1560–6
[14] Booker G R *et al* 1995 *J. Cryst. Growth.* **146** 495–502
[15] Tian Y and Zhang B *et al* 1996 *Rare Metals* **15** 172
[16] Hecht E and Zajac A 1976 *Optics* 1st edn (Reading MA: Addison-Wesley)
[17] Kishino K and Selim Ünlü M *et al* 1991 *IEEE J. Quantum Electron.* **27** 2025–34
[18] Sai-Halosz G A, Esaki L and Harrison W A 1978 *Phys. Rev.* B **18** 2812–8
[19] Adachi S 1989 *J. Appl. Phys.* **66** 6030–40
[20] Fang R-C 2001 *Solid State Spectroscopy* (Hefei: University of Science and Technology of China Press)
[21] JITA 1973 *Compound Semiconductor Devices and III–V Compound Semiconductor Basic Parameters* (Tokyo: Japan Industrial Technology Association)